JOURNAL OF THE ROYAL SOCIETY Interface

Shearing of fibrillar adhesive microstructure: friction and shear-related changes in pull-off force

M Varenberg and S Gorb

J. R. Soc. Interface 2007 **4**, 721-725
doi: 10.1098/rsif.2007.0222

JOURNAL OF THE ROYAL SOCIETY Interface

J. R. Soc. Interface (2007) **4**, 721–725
doi:10.1098/rsif.2007.0222
Published online 27 February 2007

Shearing of fibrillar adhesive microstructure: friction and shear-related changes in pull-off force

M. Varenberg* and S. Gorb

Department of Thin Films and Biological Systems, Max Planck Institute for Metals Research, Heisenbergstrasse 3, Stuttgart 70569, Germany

To characterize the effect of shearing on function of fibrillar adhesive microstructure, friction and shear-related changes in pull-off force of a biomimetic polyvinylsiloxane mushroom-shaped fibrillar adhesive microstructure were studied. In contrast to a control flat surface, which exhibited pronounced stick–slip motion accompanied with high friction, the fibrillar microstructure demonstrated a stable and smooth sliding with a friction coefficient approximately four times lower. The structured contact also manifested zero pull-off force in a sheared state, while the flat surface exhibited highly scattered and unreliable pull-off force when affected by contact shearing. It appears that the fibrillar microstructure can be used in applications where a total attachment force should be generated in a binary on/off state and, most surprisingly, is suitable to stabilize and minimize elastomer friction.

Keywords: biomimetics; surface patterning; shearing; friction; adhesion

1. INTRODUCTION

Natural systems hide a virtually endless potential of technological ideas for the development of new smart-performance surfaces and materials (Scherge & Gorb 2001; Gorb 2006), and detailed studies of nature's tribological solutions have become the focus of inter-disciplinary scientific attention in recent years. The principles of contact splitting characterizing various natural attachment systems have been intensively discussed in several publications (Arzt *et al.* 2003; Persson 2003; Persson & Gorb 2003; Chung & Chaudhury 2005; Gao *et al.* 2005; Varenberg *et al.* 2006*a*) and, following extensive studies of biological fibrillar systems, few attempts have been made to produce artificial patterned adhesives (Geim *et al.* 2003; Ghatak *et al.* 2004; Glassmaker *et al.* 2004; Majidi *et al.* 2004; Peressadko & Gorb 2004; Crosby *et al.* 2005; Northen & Turner 2005; Yurdumakan *et al.* 2005). However, the reported surfaces exhibited limited life cycle and overall gain in adhesion.

Based on the analysis of the functional morphology of the tarsal hairs found in numerous species of beetles from the family Chrysomelidae, an advanced biomimetic mushroom-shaped fibrillar adhesive microstructure has been recently fabricated (Gorb *et al.* 2007). Initial testing revealed that the adhesive properties and the tolerance to contamination of this microstructure were much more effective than those of a control flat surface made of the same soft synthetic polymer. However, the tests conducted did not examine the effect of shearing, which may become significant in using this material under field conditions. In addition, despite the well-known fact that the animals possessing fibrillar attachment systems frequently use shear motion to either enhance or eliminate adhesion (Autumn *et al.* 2000; Gorb 2001; Niederegger & Gorb 2003; Autumn *et al.* 2006), the sliding behaviour of artificial fibrillar surfaces has only recently started to be investigated (Daltorio *et al.* 2005; Majidi *et al.* 2006). In light of the above, the purpose of the present work was to study friction and shear-related changes in pull-off force resulting from the shearing of biomimetic mushroom-shaped fibrillar adhesive microstructure.

2. EXPERIMENTAL DETAILS

The tests were performed on a home-made micro-tribometer that consists of motorized translation stages M-011 (Physik Instrumente GmbH, Karlsruhe, Germany) and fixed tensometric force transducers FORT-100 (World Precision Instruments Inc., Sarasota, Florida), whose bending in normal and lateral directions is used to determine the applied and friction forces with a resolution of 0.1 mN (figure 1). The force transducers were calibrated with known precise weights immediately prior to testing. To guarantee full contact during measurements in a flat-on-flat contact scheme essential in surface texture testing, a passive self-aligning system of specimen holders was used (Varenberg *et al.* 2006*b*). Specimens tested were flat and structured (figure 2; Gottlieb Binder GmbH, Holzgerlingen, Germany) polyvinylsiloxane (PVS) discs

*Author for correspondence (varenberg@mf.mpg.de).

Received 20 December 2006
Accepted 1 February 2007

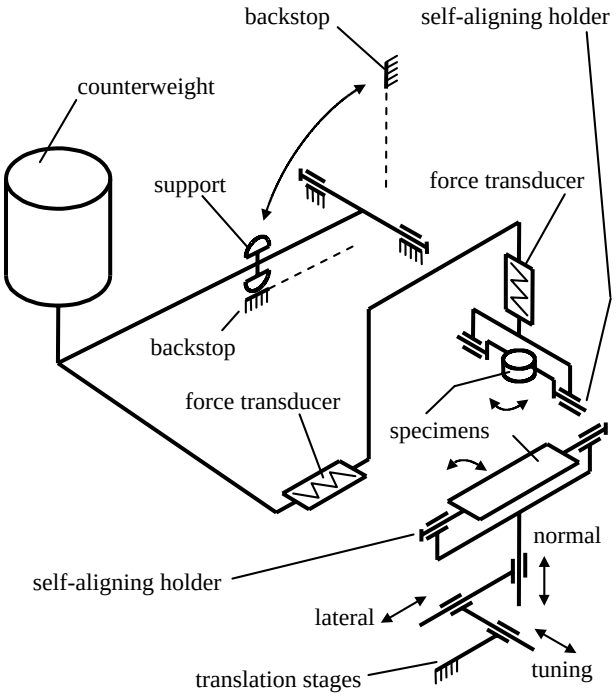

Figure 1. Schematic of the microtribometer.

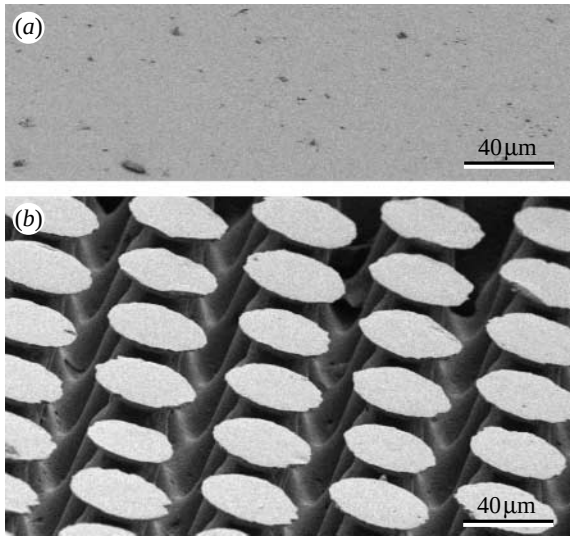

Figure 2. Contact surface of (*a*) flat and (*b*) structured PVS specimens.

of 2 mm in diameter and 1 mm in height mounted on the force transducer. A glass slide of $18\times7\times0.2$ mm^3 size fixed on the translation stage was used as a substrate. Structured surface consisted of uniformly distributed mushroom-shaped pillars of approximately 100 µm in height bearing terminal contact plates of approximately 40 µm in diameter (Gorb *et al.* 2007). The area density of the terminal contact plates was approximately 40%. The roughness average (R_a) of the glass and PVS surface was approximately 1 and 85 nm, respectively. Before the experiments, the specimens were washed with deionized water and liquid soap and then dried in flowing nitrogen. The temperature and relative humidity in the laboratory were 24°C and 41%, respectively.

Each test started by bringing the PVS specimens in contact with the glass substrate. After applying a normal load of 40, 80, 120 or 160 mN, the translation stage was moved in the lateral direction at a velocity of 100 µm s^{-1} for distances ranging from 25 µm to 7 mm, while the tangential force resisting the specimen motion was measured. Immediately before completing the lateral motion, the contact area was imaged with a monochrome digital camera M4+CL (JAI Co., Yokohama, Japan) enhanced by high-magnification optics Zoom-12X (Navitar, Inc., Rochester, New York) in order to examine the contact behaviour in shearing. Finally, the pull-off force affected by shearing of the contact zone was measured while withdrawing the translation stage in a vertical direction at a velocity of 100 µm s^{-1}.

The output signals from the microtribometer were acquired with a multifunctional data acquisition board PCI-6251 (National Instruments Co., Austin, Texas). The translation stages were controlled in a closed-loop manner with a stepper/servo motion controller PCI-7344 (National Instruments Co.). The contact images were obtained with an image acquisition board PCI-1428 (National Instruments Co.). To provide online monitoring of the contact response, all data were processed with a LabVIEW software package.

3. RESULTS AND DISCUSSION

Figure 3 shows representative friction curves obtained as a function of lateral stage displacement under an applied load of 40 mN. The difference in sliding behaviour of flat and structured surfaces becomes obvious. The flat surface exhibited pronounced stick–slip motion (figure 3*a*), which was rather similar to specimen jumps and associated with complete detachment of the PVS surface from the glass substrate. These jumps presumably arise from the self-aligning ability of the contacting surfaces and considerably differ from the 'waves of detachment' (Schallamach 1971), characterizing relative motion of fixed elastomer surfaces. This behaviour was clearly identified by optical inspection of the contact zone during the tests, as destructive interference of reflected white light in the glass–PVS interface resulted in visualization of the real contact area. Inserts *a*1–*a*4, where the dark grey zone corresponds to the real contact and the zones coloured from light grey to white are non-contact regions, demonstrate changes in contact area during one gross stick–slip event. Insert *a*1 presents an initial contact. No relative movement of the contacting surfaces is observed between the specimen jumps, and growing elastic stresses during the stick phase of motion result in reduction of a real contact area only (inserts *a*2, *a*3). After each jump, the surface comes in contact at different stress conditions that lead to differences in appearance of the real contact area (inserts *a*3, *a*4).

In contrast to the flat surface, the structured one demonstrated a stable and smooth sliding (figure 3*b*) characterized by a significantly lower lateral force needed to initiate a relative motion between the contacting surfaces, which is in agreement with the preliminary results reported earlier (Daltorio *et al.* 2005). The microstructured contact behaviour during

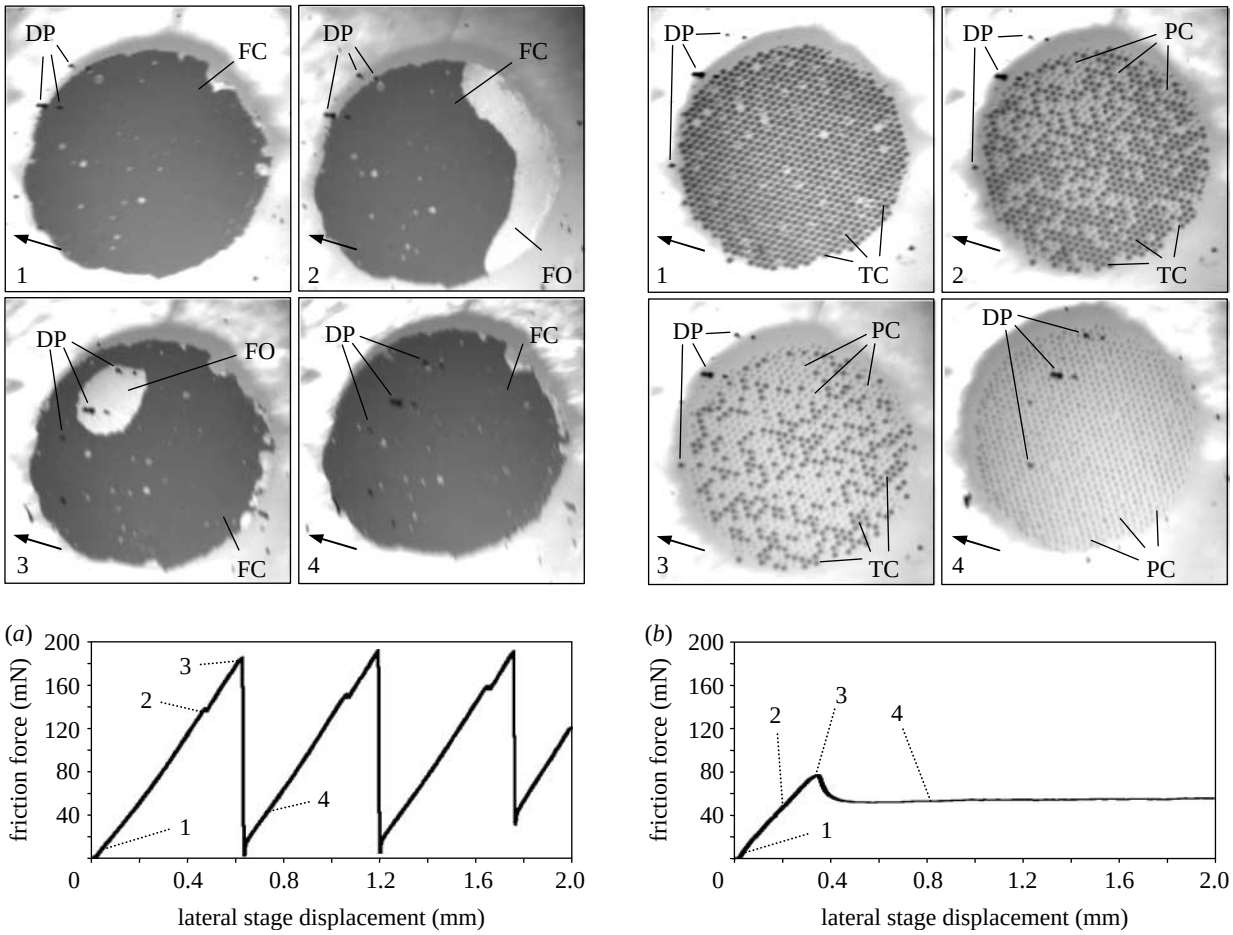

Figure 3. Friction force of (*a*) flat and (*b*) structured specimens measured as a function of lateral stage displacement under an applied load of 40 mN. Inserts *a*1, *a*2, *a*3 and *a*4 are images of flat contact area made after lateral displacements of 60, 460, 620 and 720 µm, respectively. Inserts *b*1, *b*2, *b*3 and *b*4 are images of structured contact area made after lateral displacements of 60, 200, 350 and 820 µm, respectively. DP, dust particles; FC, flat surface in contact; FO, flat surface out of contact; TC (dark grey spots), terminal plates in contact; PC (grey spots), bent pillars in contact; arrows in the direction of specimen motion.

sliding is depicted in inserts *b*1–*b*4, where the first three images demonstrate an initial transient period and the last one presents the steady-state motion. It is shown that the flat plates terminating the structured surface gradually lose their contact with the glass substrate until the real contact area becomes much smaller and the whole contact starts sliding. A growing tangential load produced by the contact shearing is accommodated by bending of individual pillars, which bear the normal load on their edges when the terminal plates tend to come out of the contact (figure 4). Interestingly, every pillar is independent of its neighbours and, despite individual pillars possibly experiencing sliding irregularities, their collective motion results in a smooth sliding of the entire surface due to a random distribution and small amplitude of single stick–slip events. Through a significant decrease in real contact area (figure 3*b*, inserts 1–4; figure 4), which determines the actual friction force (Parker & Hatch 1950), an individual pillar bending is also believed to contribute to a reduction in the static friction observed with the structured surface. This is the opposite of the microfibre arrays constructed from a stiff polypropylene, where the microstructure deformation leads to an increase in real contact area and the fibre arrays show more than

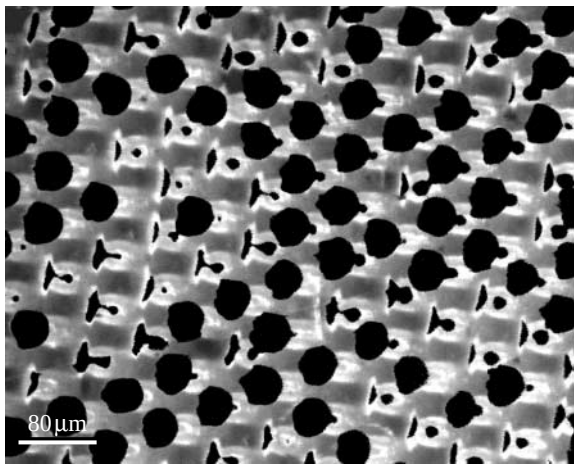

Figure 4. Sheared PVS microstructure in contact with a flat glass substrate. Black areas are the real contact zones formed by both terminal plates and stalks of bent pillars.

an order of magnitude increase in friction compared with the bulk material (Majidi *et al.* 2006).

Figure 5 depicts static friction force of flat and structured specimens measured as a function of applied load. The friction force is linear with respect to the applied load in both the cases, while the flat surface

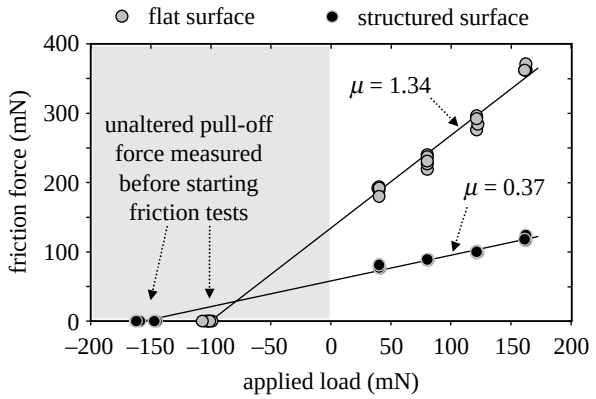

Figure 5. Static friction force of flat and structured specimens measured as a function of applied load.

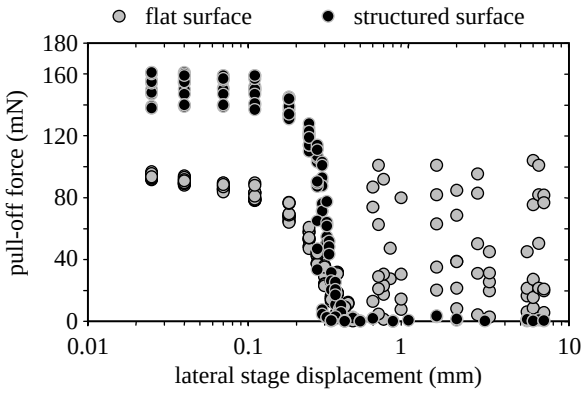

Figure 6. Pull-off force of flat and structured specimens affected by contact shearing under applied loads of 40, 80, 120 and 160 mN and measured as a function of lateral stage displacement.

demonstrates much higher friction. It is worth noting that the friction force measured with the flat specimens is probably underestimated. The reason is that the self-aligning holders suspended on threads (Varenberg *et al.* 2006*b*) give to the specimens some freedom to move in normal direction and hence the specimens can jump before the contact is actually sheared. The friction coefficient μ, which is defined as a ratio of the friction force to the sum of the applied load and the pull-off force, is actually the slope of the friction–load line. It was fitted with the coefficient of determination R^2 of 0.99 and found to be 1.34 and 0.37 for flat and structured surfaces, respectively. The pull-off force presented in this figure was determined before the friction tests and, according to the previous reports (Varenberg *et al.* 2006*a*,*b*), was found to be independent of maximum applied load in a loading cycle.

Figure 6 shows pull-off force of flat and structured specimens affected by contact shearing under applied loads of 40, 80, 120 and 160 mN and measured as a function of lateral stage displacement. Shearing of both flat and structured surfaces initially led to reduction in the pull-off force, which approached zero at the lateral stage displacement of approximately 500 μm. With additional increase in lateral displacement, the pull-off force scattered between its unaltered value and zero on flat surfaces and remained zero on structured surfaces. Interestingly, despite presumably different physics in shearing of flat and structured surfaces, both the studied types of specimens lose an ability to resist pull-off forces after approximately the same critical lateral displacement. This, however, can be explained by the fact that deformation of the specimens and their holders accommodates a relatively large lateral displacement, while the difference in real interface displacement of flat and structured surfaces cannot be seen on this scale.

A gradual loss of ability to resist pull-off forces with the application of a tangential load to the flat surface is connected to the stick–slip motion. No relative movement can be initiated in a large flat contact, while adhesive bonds between PVS and glass can withstand indefinitely a certain maximum tangential stress. Hence, the closer is the contact to the point at which the adhesive bonds are ruptured and the surface detachment occurs, the smaller is the additional pull-off force needed to withdraw the specimen from the contact. This is directly confirmed by figure 3*a*, where some stick–slip event can be seen at the lateral stage displacement of approximately 500 μm characteristic of a complete loss of ability to resist pull-off forces. The pull-off force measured at larger lateral displacements is scattered for the same reason, as after each detachment the surface jumped in contact at different tangential stress conditions that led to differences in withdrawal forces.

The mechanism of pull-off force reduction in the structured contact (figure 6) is most probably defined by pillar bending, which increases with the lateral stage displacement until attaining a certain level determined by a static friction force and remains constant after sliding inception. The degree of pillar bending is reflected in a gradual reduction of the contact zone (figure 3*b*, inserts 1–4) and storage of additional elastic energy working against adhesion. This directly affects the pull-off force, which is finally turned off at a definite lateral displacement. Interestingly, symmetric design of mushroom-shaped pillars leads to bending isotropy and does not allow controlled peeling of individual contact elements. Therefore, the pull-off force decreases independently of the direction of shearing. This is in contrast to asymmetric peeling-oriented spatula-shaped adhesive outgrowths found in attachment organs of different animals (Autumn *et al.* 2000; Gorb 2001; Gao *et al.* 2005), which control attachment forces by shearing the contact in different directions, thus changing the peeling angle of terminal contact elements (Niederegger & Gorb 2003; Autumn *et al.* 2006).

4. CONCLUSION

The tests performed show that from the viewpoint of both frictional and adhesive properties defined by contact shearing, the structured surface behaves in a much more predictable and simple way than the flat one, thus expanding the potential of this surface texturing. It appears that the fibrillar microstructure can also be used in applications where a total attachment force should be generated in a binary on/off state and, most surprisingly, is suitable to stabilize and minimize elastomer friction.

S.G. was supported in this work by the Federal Ministry of Education, Science and Technology, Germany (project InspiRat 01RI0633C).

REFERENCES

Arzt, E., Gorb, S. & Spolenak, R. 2003 From micro to nano contacts in biological attachment devices. *Proc. Natl Acad. Sci. USA* **100**, 10 603–10 606. (doi:10.1073/pnas.1534701100)

Autumn, K., Liang, Y. A., Hsieh, S. T., Zesch, W., Chan, W. P., Kenny, T. W., Fearing, R. & Full, R. J. 2000 Adhesive force of a single gecko foot-hair. *Nature* **405**, 681–685. (doi:10.1038/35015073)

Autumn, K., Dittmore, A., Santos, D., Spenko, M. & Cutkosky, M. 2006 Frictional adhesion: a new angle on gecko attachment. *J. Exp. Biol.* **209**, 3569–3579. (doi:10.1242/jeb.02486)

Chung, J. Y. & Chaudhury, M. K. 2005 Roles of discontinuities in bio-inspired adhesive pads. *J. R. Soc. Interface* **2**, 55–61. (doi:10.1098/rsif.2004.0020)

Crosby, A. J., Hageman, M. & Duncan, A. 2005 Controlling polymer adhesion with "pancakes". *Langmuir* **21**, 11 738–11 743. (doi:10.1021/la051721k)

Daltorio, K. A., Gorb, S., Peressadko, A., Horchler, A. D., Ritzmann, R. E. & Quinn, R. D. 2005 A robot that climbs walls using micro-structured polymer feet. In *Proc. Int. Conf. Climbing and Walking Robots, London, UK*, pp. 131–138.

Gao, H. J., Wang, X., Yao, H. M., Gorb, S. & Arzt, E. 2005 Mechanics of hierarchical adhesion structures of geckos. *Mech. Mater.* **37**, 275–285. (doi:10.1016/j.mechmat.2004.03.008)

Geim, A. K., Dubonos, S. V., Grigorieva, I. V., Novoselov, K. S. & Zhukov, A. A. 2003 Microfabricated adhesive mimicking gecko foot-hair. *Nat. Mater.* **2**, 461–463. (doi:10.1038/nmat917)

Ghatak, A., Mahadevan, L., Chung, J. Y., Chaudhury, M. K. & Shenoy, V. 2004 Peeling from a biomimetically patterned elastic film. *Proc. R. Soc. A* **460**, 2725–2735. (doi:10.1098/rspa.2004.1313)

Glassmaker, N. J., Jagota, A., Hui, C.-Y. & Kim, J. 2004 Design of biomimetic fibrillar interfaces: 1. Making contact. *J. R. Soc. Interface* **1**, 23–33. (doi:10.1098/rsif.2004.0004)

Gorb, S. N. 2001 *Attachment devices of insect cuticle*. New York, NY: Springer.

Gorb, S. N. 2006 Functional surfaces in biology: mechanisms and applications. In *Biomimetics: biologically inspired technologies* (ed. Y. Bar-Cohen), pp. 381–397. Boca Raton, FL: CRC Press.

Gorb, S., Varenberg, M., Peressadko, A. & Tuma, J. 2007 Biomimetic mushroom-shaped fibrillar adhesive microstructure. *J. R. Soc. Interface* **4**, 271–275. (doi:10.1098/rsif.2006.0164)

Majidi, C., Groff, R., & Fearing, R. 2004 Clumping and packing of hair arrays manufactured by nanocasting. In *Proc. ASME IMECE*, 62142.

Majidi, C. *et al.* 2006 High friction from a stiff polymer using microfiber arrays. *Phys. Rev. Lett.* **97**, 076 103. (doi:10.1103/PhysRevLett.97.076103)

Niederegger, S. & Gorb, S. 2003 Tarsal movements in flies during leg attachment and detachment on a smooth substrate. *J. Insect Physiol.* **49**, 611–620. (doi:10.1016/S0022-1910(03)00048-9)

Northen, M. T. & Turner, K. L. 2005 A batch fabricated biomimetic dry adhesive. *Nanotechnology* **16**, 1159–1166. (doi:10.1088/0957-4484/16/8/030)

Parker, R. C. & Hatch, D. 1950 The static coefficient of friction and the area of contact. *Proc. Phys. Soc. B* **63**, 185–197. (doi:10.1088/0370-1301/63/3/305)

Peressadko, A. & Gorb, S. N. 2004 When less is more: experimental evidence for tenacity enhancement by division of contact area. *J. Adhes.* **80**, 1–15. (doi:10.1080/00218460490430199)

Persson, B. N. J. 2003 On the mechanism of adhesion in biological systems. *J. Chem. Phys.* **118**, 7614–7621. (doi:10.1063/1.1562192)

Persson, B. N. J. & Gorb, S. 2003 The effect of surface roughness on the adhesion of elastic plates with application to biological systems. *J. Chem. Phys.* **119**, 11 437–11 444. (doi:10.1063/1.1621854)

Schallamach, A. 1971 How does rubber slide? *Wear* **17**, 301–312. (doi:10.1016/0043-1648(71)90033-0)

Scherge, M. & Gorb, S. N. 2001 *Biological micro- and nanotribology: nature's solutions*. Berlin, Germany: Springer.

Varenberg, M., Peressadko, A., Gorb, S. & Arzt, E. 2006*a* Effect of real contact geometry on adhesion. *Appl. Phys. Lett.* **89**, 121 905. (doi:10.1063/1.2356099)

Varenberg, M., Peressadko, A., Gorb, S., Arzt, E. & Mrotzek, S. 2006*b* Advanced testing of adhesion and friction with a microtribometer. *Rev. Sci. Instrum.* **77**, 066 105. (doi:10.1063/1.2214692)

Yurdumakan, B., Raravikar, N. R., Ajayan, P. M. & Dhinojwala, A. 2005 Synthetic gecko foot-hairs from multiwalled carbon nanotubes. *Chem. Commun.* **30**, 3799–3801. (doi:10.1039/b506047h)